Journal of Genetics, Genomics & Plant Breeding 9(2) 42-54 (April, 2025)
ISSN (Online): 2581-3293 DOI:10.63551/jggpb.vol.9.issue02.002

RESEARCH ARTICLE

In vivo betacyanin expression via agrobacterium-mediated 35S-RUBY plasmid delivery enhances photosynthetic efficiency and carbon dioxide sequestration in *Lactuca sativa*

V. Yarlagadda

Arizona College Preparatory High School, 4477 South Gilbert Dr, Chandler, AZ, 85286, United States of America

Corresponding authors email: vy88neuro@gmail.com

Manuscript received: March 27, 2025; Decision on manuscript, April 12, 2025; Manuscript accepted: April 13, 2025

Abstract

The focus of this research was to mitigate the absorption of high-energy wavelengths through the insertion of the 35S RUBY plasmid, which contains the genes necessary for Betacyanin synthesis. To evaluate potential benefit of betacyanin expression, a three-pronged assay evaluating absorbance, CO_2 assimilation, and biomass proportion was employed to determine differences in photosynthetic potential in *Lactuca sativa* plants that were transformed with the 35S RUBY plasmid. The 35S RUBY plasmid coded for an enzyme pathway which converts excess cytoplasmic tyrosine to betacyanin. As a result, visible pigmentation formed on injection sites of chosen plants. After a thorough spectrophotometric analysis of tissue samples along the photosynthetic activity range, both injected and non-injected plants were studied to determine the rate at which CO_2 levels decreased in airtight environments. It was found that plants that were injected with the RUBY plasmid absorbed carbon dioxide at a rate 37.25% (ppm/min) greater than non-treated counterparts. To evaluate the validity of the observed differences in carbon dioxide absorption, each sample group was subject to controlled heat exposure, allowing for dry-weight acquisition. Our results offer a sustainable increase to photosynthesis, which is translatable to in-field use. This approach serves to democratize carbon capture by reducing the demand for energy and complex machinery.

Keywords: *Lactuca sativa*, agrobacterium-mediated transformation, RUBY plasmid, CO_2 sequestration, Betacyanin

Introduction

Globally, CO_2 emissions have increased by 60% since 1990 (Tiseo, 2025). Despite the urgency to meet net-zero carbon emissions by 2050, there is an unmet need for sustainable CO_2 sequestration methods. CO_2 sequestration, a negative emissions process, involves the direct acquisition of CO_2 from the air. Direct Air Carbon Capture (DACC), a motorized process of CO_2 removal, has become the focus of modern-day sequestration technology. DACC relies on large fans, and chemical processes such as adsorption or absorption to sequester CO_2. From the point of CO_2 recruitment, energy must be applied to store CO_2 that is absorbed or adsorbed by reagents used in carbon capture. However, the high energy requirements and underground storage of CO_2 inhibit the rollout of DACC. Without a strong renewable energy network, DACC will ultimately contribute to the continued use of fossil fuel energy, and the underground storage of CO_2 augments the risk of CO_2 leakage, which can contribute to groundwater

acidification and environmental damage (Deutz and Bardow, 2021). With the potential to devastate environments and agricultural economy, DACC fails to address the global demand for CO_2 sustainably. To meet international climate targets with a continued consideration for the environment and energy expenditure, naturally sequestering processes such as photosynthesis should be employed. Photosynthesis, a process situated in either the chloroplast or prokaryotic cell, is responsible for the conversion of light to usable chemical energy in plants, certain protists, and cyanobacteria. It relies on a two-pronged system consisting of an electron transport chain and the Calvin Cycle. CO_2 is sequestered during the Calvin Cycle, when it is conjoined with Ribulose Biphosphate 1,5 (a cycle intermediate). However, the quantum efficiency of photosynthesis is 26%; the relatively low figure has spurred multiple investigations. Increasing the efficiency of photosynthesis has been a growing area of research in plant genomics, coinciding with the advent of precise gene editing technologies. Current efforts to improve photosynthetic efficiency can be characterized by improving the absorption spectra of the photosynthetic electron transport chain or the synthesis of Rubisco in the Calvin Cycle. However, these investigations fail to address a key limitation of photosynthesis: the potential for inhibition due to the metabolic imbalance between the photosynthetic electron transport chain and the Calvin Cycle. Excessive interaction with light in the photosystems may create products at a rate faster than they can be assimilated by the Calvin Cycle, creating a demand for alternative electron quenching methods. A potential pathway is the return of electrons to oxygen gas, which results in the production of singlet oxygen, a high-energy reactive oxygen species that contributes to significant oxidative damages (Barta *et al.*, 2004). Photosynthetic inhibition coincides with the accumulation of reactive oxygen species (ROS), which cause oxidative damage due the metabolic imbalance between the production of electron-dependent molecules and their use in the Calvin Cycle. This metabolic imbalance, which perpetuates ROS accumulation, occurs when an excess of high-energy wavelengths is absorbed by photosynthetic antennae (Goh *et al.*, 2011). Reactive oxygen species (ROS) are synthesized throughout a variety of metabolic processes that occur in the cell. In photosynthesis, they are generated when high-energy electrons cannot be quenched through the electron transport chain. Photosynthesis is initiated by photonic excitation of electrons situated in pigment molecules such as chlorophyll. The energy absorbed is quenched by the electron transport chain, which uses the high-energy electrons to create a proton gradient for ATP synthesis. After the initial excitation has been quenched by electron carrier movement and proton displacement, the electrons are re-excited in Photosystem 1. This helps create high-energy electron carriers such as Nicotinamide Adenine Dinucleotide Phosphate (NADPH), the terminal product of the photosynthetic electron transport chain. The electrons in Photosystem 2, the site of initial excitation, are replenished by the photolysis (split) of water molecules in the thylakoid lumen. Cumulatively, this process is known as photochemical quenching (qE), where the electron transport chain is successfully employed to quench electrons. In the case of metabolic imbalance, qE cannot be pursued. This necessitates pathways such as cyclic electron flow around Photosystem 1 or non-photochemical quenching to quench electrons. These pathways aim to return electrons to their ground state through cyclic electron flow, which prevents the over-reduction of $NADP^+$. Additionally, the violaxanthin cycle in non-photochemical quenching (NPQ) synthesizes zeaxanthin to dissipate excess energy carried by high-energy electrons (Hasanuzzaman *et al.*, 2020). Despite the existence of these mitigative pathways in photosynthesis, when the electron transport chain becomes over-reduced, ROS synthesis is nearly imminent.

In Photosystem 2, excitation creates triplet chlorophyll, when two electrons possess the same spin. Without suitable quenching, the electrons are passed to oxygen, resulting in the synthesis of species such as superoxide radicals or singlet oxygen (Hasanuzzaman *et al.*, 2020). When such species surpass the antioxidant capacity of antioxidant defense systems, a combination of chemical species and enzymes that have ROS scavenging properties, oxidative damages can occur. ROS are capable of chemically deactivating Photosystem 2, resulting in photoinhibition. Reactive oxygen species cause oxidative damages to the amino acids of D1 Protein in the Reaction Center Complex of Photosystem 2. The D1 protein is instrumental to the stabilization and function of the OEC, particularly the Mn_4CaO_5 cluster, which is crucial to recruiting electrons necessary for photosynthesis. The D1 protein is terminal to the OEC, and therefore is subject to oxidation during excessive ROS activity. This ultimately triggers the proteolysis of D1, a hallmark of photoinhibition. Besides photoinhibition, ROS are highly potent molecules that can result in the peroxidation of phospholipids in the lipid bilayer and DNA. This can result in membrane liquefaction and apoptosis in extreme cases. The focus of this research was to mitigate the absorption of high-energy wavelengths through the insertion of the 35S RUBY plasmid, which contains the genes necessary for Betacyanin synthesis. Betacyanin is a phenolic compound that possesses ultraviolet-absorbing and ROS-quenching properties. Ultraviolet, blue, red, and green wavelengths are known stress regions of the electromagnetic spectrum, meaning they are more likely to trigger metabolic imbalance and ROS synthesis (Barta *et al.*, 2004). The capability to prevent oxidative damage is instrumental to photosynthetic capability. Betacyanin, which is a member of the Betalain family, is a pigment that is commonly found in Beta vulgaris and various other edible species of Caryophyllales (Sadowska-Bartosz and Bartosz, 2021). Although this pigment's original composition originates from various members of the Caryophyllales, the photosynthetic capabilities of these pigments are largely untapped, because the pigment is produced in non-photosynthetic bodies of plants. The method proposed by this work utilizes bacterial conjugation, specifically *Agrobacterium tumefaciens*, to deliver the 35S RUBY plasmid. Genes coding for the enzymes Glucosyltransferase, Cytochrome P450, and 4,5 DOPA Dioxygenase were incorporated in the plasmid and administered to a subset of the Lactuca sativa plants studied. These specific enzymes are integral to the Betalain biosynthesis pathway and the production of Betacyanin. The condensation of Betalamic acid with cyclo-DOPA in betalains widens the electronic resonance of the diphenol aromatic ring. This extra conjugation results in a bathochromic effect, shifting the absorption maximum from about 480 nm, typical of betaxanthins (yellowish betalains), to the region of about 540 nm (Sadowska-Bartosz and Bartosz, 2021). Betacyanins have the potential to be advantageous to photosynthetic processes are due to its biochemical structure. The condensation process, which is pictured below, depicts the process by which Betalamic acid, the primary chromophore of Betalains, and cyclo-DOPA condense to form Betacyanins (Sadowska-Bartosz and Bartosz, 2021). Betacyanins also undergo a glucosylation process that pulls electron density from the aromatic ring. This necessitates high energy wavelengths for excitation, contributing to the UV absorption maxima found in betacyanins. The difference in the following work and other research in photosynthetic enhancement involves the methodology behind improving efficiency. This research aims to determine whether the absorbance spectrum of betacyanin, specifically at inhibitory regions of the electromagnetic spectrum, can improve photosynthetic efficiency by screening harmful wavelengths. This approach evolved into the present investigation aimed to evaluate a potential benefit of betacyanin expression.

ISSN (Online): 2581-3293 DOI:10.63551/jggpb.vol.9.issue02.002

Materials and methods

Plant transformation materials and *Agrobacterium tumefaciens* delivery and plasmid expression

A total of 12 *Lactuca sativa* (n=12) plants were studied in this work. 6 of these plants were injected administered with an *A tumefaciens* injection media. The other 6 plants did not receive any treatment, establishing a clear treatment and control group. The photosynthetic benefit of the pigment was evaluated using a three-pronged methodology that involved a spectrophotometric comparison of homogenized plant tissue, a closed-chamber CO_2 assimilation analysis, and a biomass acquisition. These assays test for external indicators of photosynthesis and distinguish potential differences in efficiency due to betacyanin expression. 18 vials of 50µl freeze dried *A. tumefaciens* possessing the 35S RUBY plasmid were cultured on 36 Agar Rif/Spec plates. Conventionally, *A. tumefaciens* infects plants with Crown-Gall disease, an infection that presents tumor-like growths. In most cases, the Tumor inducing (Ti) plasmid is cleaved into nucleic DNA instead of being delivered to the cytoplasm. The 35S RUBY plasmid was delivered using the Binary Bacterial Artificial Chromosome (BiBAC) system, which involves the use of the *A. tumefaciens* secretion system to deliver foreign DNA (Jaboulay *et al.*, 2022). Blunt syringe administration discussed by Chincinska (2021) was used in this study. Upon successful delivery of the 35S RUBY plasmid, the genes necessary Betacyanin biosynthesis were expressed. According to isotope tagging, enzymes on the 35S RUBY plasmid are primary localized to the cytoplasm (Chen *et al.*, 2017). Despite the cytoplasmic localization of the associated enzymes, Betacyanin is localized to the central vacuole like many other secondary pigments. The mechanism of this localization is unknown, however it is predicted that Betacyanin enters the central vacuole through ATP Binding Cassette (ABC) proteins. Anthocyanins, a more common structural relative of Betacyanins, are deposited into the central vacuole through ABC proteins. Standard plant transformation procedures developed by Chincinska (2021) used in the present study.

Three-pronged experimentation strategy

The spectrophotometric procedures, developed by Pramanik *et al.*, (2024), were designed to quantify Betalains through a spectrophotometric analysis of extracted pigment. The necessary tissue was obtained from four *L. sativa* samples (two from each sample group), which did not participate in further experimentation. An 80% acetone solution was used for the chemical extraction of pigment from plant tissues. While the absorbance values from the developed cuvettes were used for initial data, the quantification formula developed by Pramanik et al. (2024) was used to obtain a covariate for the Analysis of Covariance (ANCOVA) test. ANCOVA was conducted to ensure that pigment dispersion was not the effector of the dependent variable. CO_2 assimilation allows for a comparative analysis of the rate at which CO_2 is sequestered. This assay provides key insight into differing photosynthetic rate, considering that CO_2 is an essential reactant for the Calvin Cycle. The CO_2 assimilation procedure was developed by the author, which relies on the following:

1. Obtain 2 plastic chambers fitted with a CO_2 sensor
2. Create a small reaction vessel to prevent premature photorespiration. Add 30g of $NaHCO_3$ (s) to 600 mL of 5% CH_3COOH (aq) to create carbon dioxide

3. Place the reaction vessel inside the chamber and allow levels to stabilize at roughly 1550 ppm CO_2. Seal the plant within the chamber and record the initial [CO_2]
4. For every 30 seconds during a 17 minute interval, record the concentration of CO_2 in order to determine the rate of CO_2 assimilation.
5. Repeat the assimilation test for the remaining plants in each sample group.

After the data was collected, a linear regression analysis and an unpaired t-test were used to evaluate differences in the CO_2 assimilation rate and its significance of data, respectively. To experimentally validate the results observed in the CO_2 assimilation analysis, biomass was acquired through a controlled heating process developed by the author. This heating process allowed for dry-weight (biomass) acquisition that can be cross-checked with data trends observed in prior assays.

1. Using an analytical scale and weigh boat, derive the initial plant weights.
2. Place each sample group on separate autoclave trays and divide them.
3. Set an incubator to 60°C and place the trays inside once the desired temperature is reached
4. Record the weight of each plant every 24 hours for a 96 hour period. (Timing may vary) The biomass retrieval process is complete once the weight remains consistent for a minimum of 24 hours.

After the biomass was acquired for each sample group, the dry-weight was normalized through the derivation of biomass proportion (%). This normalized unit allows for effective statistical comparison between plants of different initial weights.

Results and discussion

The focus of this research was to mitigate the absorption of high-energy wavelengths through the insertion of the 35S RUBY plasmid, which contains the genes necessary for Betacyanin synthesis. Following section discusses the results obtained in the spectrophotometric experiment. Statistically significant differences in absorption were observed in ultraviolet-b, green, blue, and far-red color ranges respectively (p value range: 0.0485-0.0033). UV, blue, and far-red wavelengths are known stressors of photosynthetic light harvesting complexes because of high affinity to photosystems in the case of blue and far-red light. UV light is high in energy, therefore is more able to readily form a triplet chlorophyll molecule. Additionally, the green light range is more likely to trigger photoinhibition in deeper tissue due to the minimal affinity of green light in photosynthetic antennae. These phenomena decrease the efficiency of photosynthesis by stressing the electron transport chain, which can lead to the formation of harmful Reactive Oxygen Species that can contribute to oxidative damage in the cell. Cuvettes containing betacyanin produced a significantly higher absorption in stressor wavelength regions. While this may produce a counterintuitive effect, the localization of betacyanin relative to chloroplasts offers photoprotective properties. According to Solovchenko and Merzlyak (2009), phenols such as betacyanin tend to accumulate in the mesophyll and upper epidermis tissue. These pigments, located adjacent or above chloroplasts, enable screening properties that contribute to photo protectivity. Further supporting filtration, Wargent *et al.*, (2011) found that using UV-opaque films over photosynthesis sites in L. sativa increased net photosynthesis by 18-21% in field and controlled environments respectively. Particularly, research has shown that exclusion of UV-B wavelengths in C_3 and C_4 plants increased Rubisco activity and resulted in increased photosynthesis (Kataria *et al.*, 2013). Notably, betacyanin excluded UV-B wavelengths in the spectrophotometric analysis

Table 1: Absorbance of betacyanin (left) vs control group (left) cuvettes at wavelengths along the Photosynthetic Activity Range (PAR)

nm	C1	C2	C3	C4	C5	nm	C1	C2	C3	C4	C5	p value
340	1.11	0.90	0.82	1.28	1.14	**340**	1.02	0.09	0.80	0.81	0.64	0.0049
380	0.48	0.59	0.57	0.64	0.52	**380**	0.59	0.45	0.32	0.6	0.57	0.3979
400	0.32	0.57	0.41	0.6	0.53	**400**	0.45	0.39	0.20	0.44	0.44	0.1868
405	0.31	0.59	0.40	0.63	0.54	**405**	0.46	0.40	0.19	0.44	0.45	0.2145
420	0.36	0.70	0.46	0.75	0.64	**420**	0.52	0.46	0.22	0.49	0.51	0.0282
435	0.4	0.78	0.50	0.83	0.72	**435**	0.57	0.48	0.24	0.51	0.56	0.0033
450	0.33	0.65	0.42	0.69	0.60	**450**	0.47	0.41	0.20	0.45	0.48	0.023
480	0.23	0.48	0.31	0.52	0.45	**480**	0.32	0.29	0.14	0.34	0.34	0.017
495	0.14	0.34	0.21	0.37	0.32	**495**	0.22	0.19	0.08	0.25	0.23	0.1593
533	0.05	0.20	0.13	0.23	0.20	**533**	0.1	0.10	0.02	0.16	0.13	0.1718
538	0.04	0.20	0.12	0.23	0.19	**538**	0.1	0.10	0.02	0.16	0.13	0.2279
570	0.05	0.20	0.12	0.23	0.19	**570**	0.1	0.09	0.02	0.16	0.13	0.1856
620	0.08	0.24	0.15	0.27	0.23	**620**	0.13	0.12	0.04	0.18	0.15	0.133
647	0.13	0.31	0.19	0.34	0.29	**647**	0.15	0.13	0.05	0.2	0.18	0.0485
650	0.11	0.29	0.17	0.32	0.27	**650**	0.16	0.14	0.06	0.21	0.18	0.1188
664	0.2	0.45	0.27	0.49	0.41	**664**	0.23	0.20	0.09	0.26	0.24	0.0048
680	0.16	0.39	0.23	0.43	0.37	**680**	0.21	0.19	0.09	0.25	0.22	0.0047
700	0.05	0.20	0.11	0.22	0.19	**700**	0.09	0.09	0.03	0.15	0.12	0.1626
720	0.06	0.18	0.14	0.2	0.17	**720**	0.06	0.06	0.02	0.12	0.10	0.0319
750	0.03	0.13	0.08	0.15	0.13	**750**	0.06	0.06	0.02	0.12	0.10	0.285
800	0.03	0.12	0.08	0.14	0.12	**800**	0.06	0.06	0.02	0.12	0.09	0.3089

The methodology pursued in this analysis presents a key limitation: pigment distribution. Pigments in plant tissue are highly dispersed in terms of density and location; therefore, homogenized samples could carry different levels of betacyanin. Therefore, differences in absorption could be due to differences in the amount of pigment or the presence of the pigment itself. An analysis of covariance (ANCOVA), a statistical analysis which considers the influence of a third variable (covariate), was coupled with a betacyanin quantification procedure to statistically validate the difference in absorbance.

ISSN (Online): 2581-3293 DOI:10.63551/jggpb.vol.9.issue02.002

Fig. 1: Average absorbance of betacyanin vs non-betacyanin cuvettes at wavelengths along the Photosynthesis Activity Range (PAR)

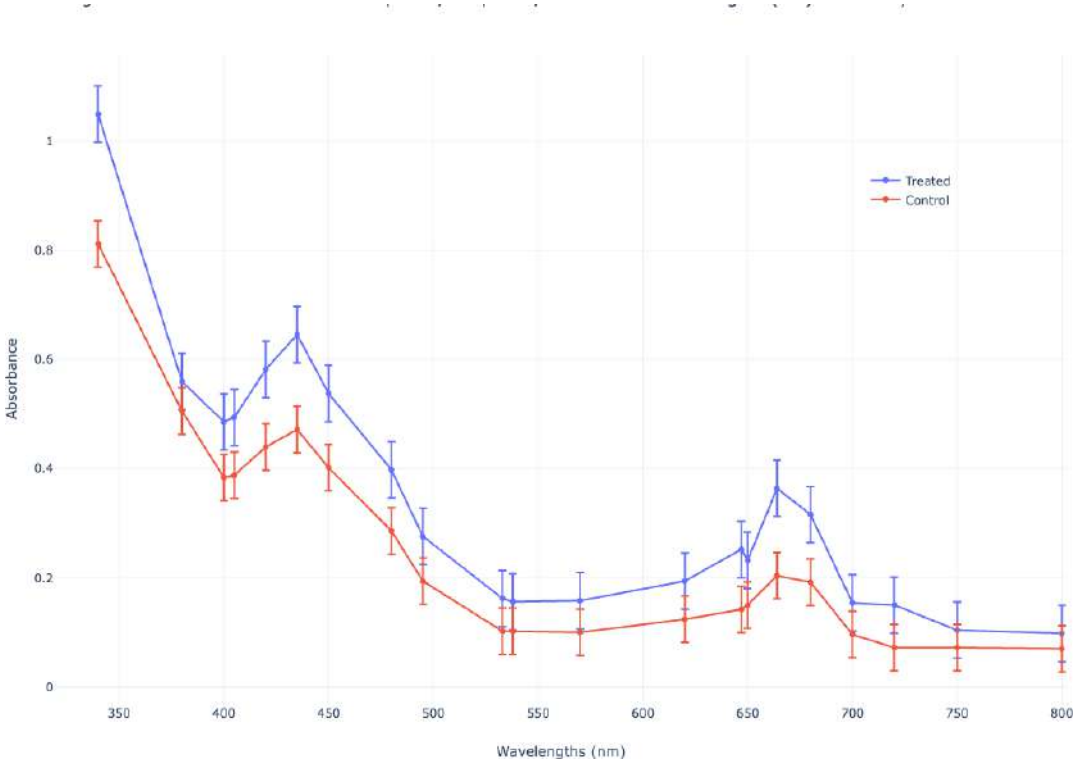

To account for this difference, the amount of betacyanin in each cuvette (mol) was quantified using the following formula (Pramanik *et al.*, 2024):

mg/kg tissue = $[(A_{538} \times 10(Dilution\ Factor) \times 550 \times 1000)/60000]$ **(1)**

Using the absorbance at 538 nm, the amount of betacyanin was quantified into mg/kg tissue. The mg/kg values were then converted into moles of betacyanin using initial weight samples of tissue. This procedure ultimately yielded the covariate, which was ultimately used to calculate ANCOVA (Table2). The F value, which is a measure of internal and external dispersion, was employed to compare the dispersion between groups and within groups. The F-values were also supplemented with p-values presented in fig 2.It is clearly discerned that at absorbance above the 380 nm wavelength possessed a significant F-value. At 340 and 380 nm, where the F-value was not statistically significant, a low signal to noise ratio likely contributed to higher numerical dispersion within the cuvettes tested at this wavelength. 340 and 380nm are situated at the minimum threshold of the spectrophotometer. Coupled with the high affinity for ultraviolet wavelengths, inconsistency in measurement likely contributed to the high level of internal dispersion at these wavelengths. However, the ANCOVA adjustment demonstrated that differences in absorption between the experimental and control group remained largely significant even with the consideration of a covariate. This demonstrates that the statistical significance of absorption was independent of betacyanin pigment concentration.

Journal of Genetics, Genomics & Plant Breeding 9(2) 42-54 (April, 2025)
ISSN (Online): 2581-3293 DOI:10.63551/jggpb.vol.9.issue02.002

Table 2: F and p values obtained from ANCOVA analysis at evaluated wavelengths

Wavelength (nm)	F (Group)	p-value (Group)	Significance
340	2.6	0.148	N/a
380	1.4	0.264	N/a
400	8.7	0.021	*
405	9.0	0.019	*
420	11.1	0.012	*
435	12.4	0.009	**
450	11.4	0.011	*
480	14.1	0.007	**
495	13.4	0.008	**
533	13.9	0.007	**
538	13.2	0.00	**
570	13.1	0.00	**
620	15.6	0.005	**
647	19.0	0.003	**
650	15.9	0.005	**
664	23.6	0.001	**
680	22.9	0.002	**
700	15.5	0.005	**
720	18.3	0.003	**
750	10.3	0.014	*
800	9.23	0.018	*

Fig. 2: F values derived from covariance Analysis (ANCOVA) of absorbance values

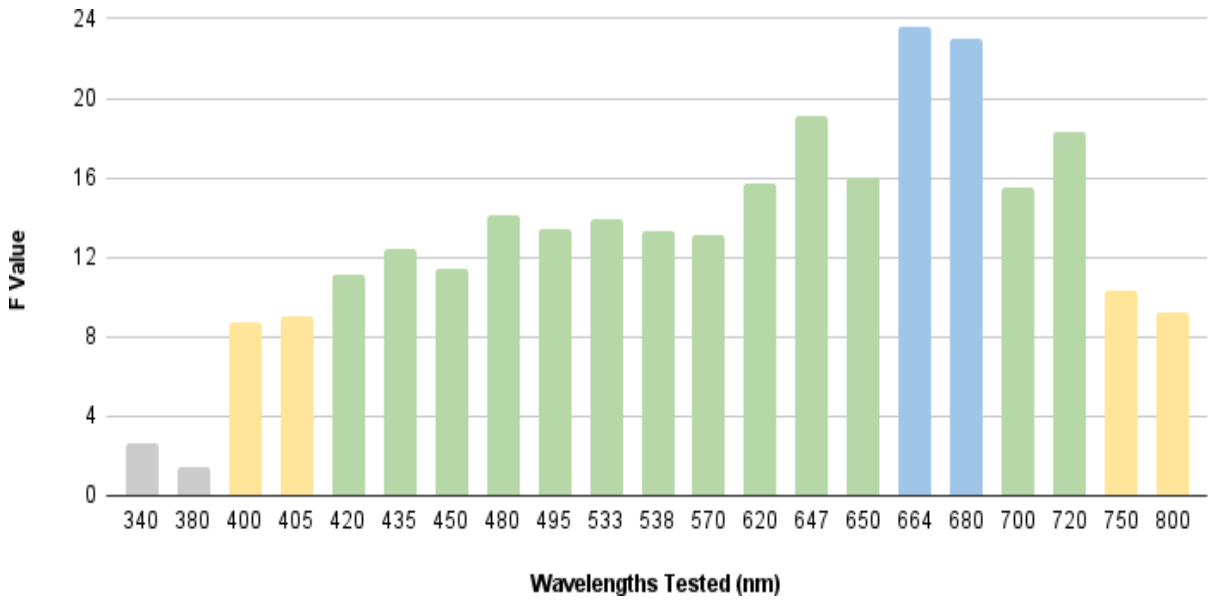

ISSN (Online): 2581-3293 DOI:10.63551/jggpb.vol.9.issue02.002

CO_2 assimilation and interpretation of the data

To evaluate the validity of the observed differences in carbon dioxide absorption, the data was run through statistical analyses which demonstrated that the data was influenced by a stimulus, such as in vivo betacyanin production. Given that CO_2 is a key reactant in the Calvin Cycle, differing sequestration rates can provide insight into differences in photosynthetic rate between the sample groups. Each plant was subjected to four trials, and the data represented below is an average of the trials performed (Table 3). The chamber [CO_2] was recorded every 30 seconds; however, the data was abridged to minute intervals for inclusion within this paper. Data on average [CO_2] Concentration ppm in chamber when subject to treated vs. non-treated plants vs. time (seconds) are presented in figure 3.

Table 3: Average chamber [CO_2] when subject to plants of the treatment and non-treatment groups

Min.	**0**	**1**	**2**	**3**	**4**	**5**	**6**	**7**	**8**
	Non-treatment group (Plant #)								
1	1551.8	1306.8	1148.3	1069.8	1026.8	1022.5	1009.8	1002	1002.5
2	1547.3	1361	1249.8	1126.5	1050.5	1007.5	997.5	1001.3	1003
3	1548.5	1380.5	1260	1162.3	1033.5	989.3	989	986.5	985
4	1553.3	1381.3	1277	1155.8	1071	1052.3	1052	1043.5	1037.5
Min.	**Non-treatment group (Plant #)**								
1	**9**	**10**	**11**	**12**	**13**	**14**	**15**	**16**	**17**
2	1002.5	992.5	983.5	978	973.3	969	967.8	967.3	961.8
3	1003	1009	1001.3	990.8	998.3	1003.5	995	997.5	994.3
4	985	980.5	982	978.5	979.3	979.8	979.8	976.3	972.8
	1037.5	1044.3	1033	1040.8	1040.5	1039	1032.8	1029.5	1034.8
	Treatment Group (Plant #)								
Min.	**0**	**1**	**2**	**3**	**4**	**5**	**6**	**7**	**8**
1	1544.5	1177.3	978.8	873.8	823	803.8	791.3	783.5	781.5
2	1540.5	1176.3	975	854	781.5	737.5	706	686	681
3	1542.3	1201	967.3	842.3	768	729.5	708	698	692.5
4	1555.5	1202.3	1004.8	895.8	819	788.8	771.8	762.3	756
Min.	**Treatment Group (Plant #)**								
1	**9**	**10**	**11**	**12**	**13**	**14**	**15**	**16**	**17**
1	777.3	769.3	762.5	766.3	766.5	768.3	768.3	771.5	772.3
2	679	680.3	675.5	673	674.3	674.3	674.8	672.3	678
3	686.3	684	684.5	688.3	685.8	697.8	686	683	694.3
4	750	747.3	744	734	735	736.3	735	727.8	727.5

Journal of Genetics, Genomics & Plant Breeding 9(2) 42-54 (April, 2025)
ISSN (Online): 2581-3293 DOI:10.63551/jggpb.vol.9.issue02.002

Fig. 3: Average [CO_2] concentration ppm in chamber when subject to treated vs. non-treated plants vs. time (seconds)

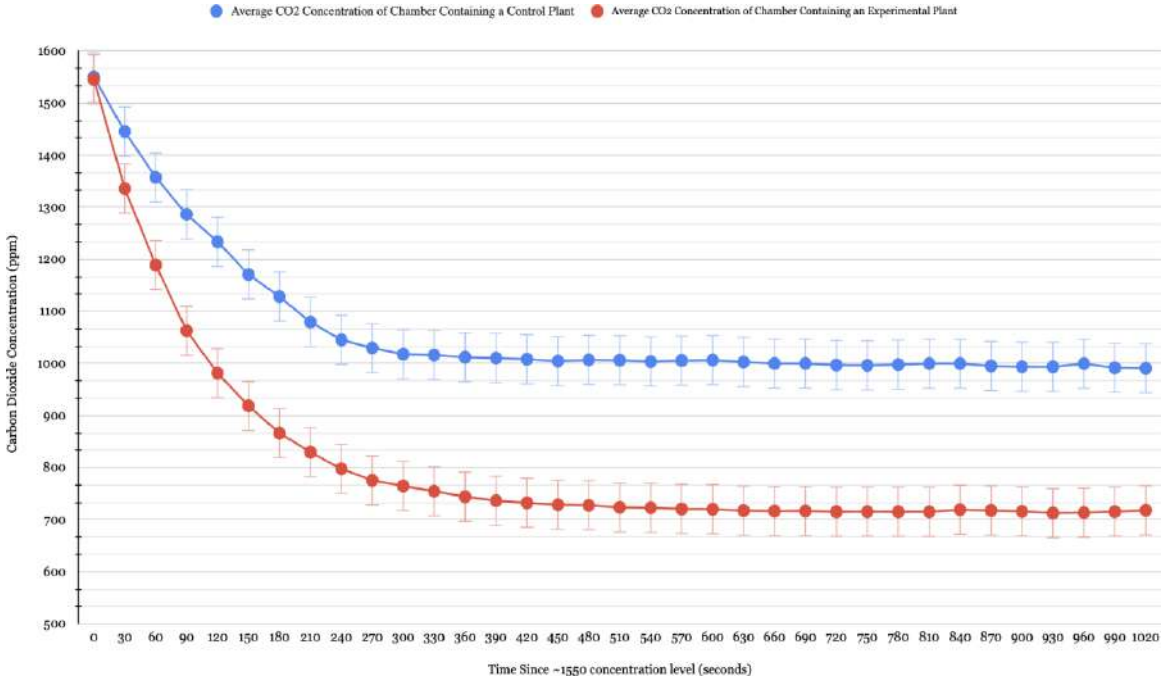

From the data above, the following equations can be derived from linear regression:

Betacyanin-producing plants: y = -28.440 x + 1064.250 **(2)**

Non-treated plants: y = -20.221 x + 1250.840 **(3)**

Linear regression models reveal that carbon dioxide concentration in a container subject to treated plants decreased at a rate of 28.440 ppm/minute (Eq. 2), while chamber [CO_2] subject to non-treated plants decreased by 20.721 ppm/minute. (Eq. 3). From the following slopes, there was a notable 37.25% increase in CO_2 assimilation when plants were administered the treatment. The average of average data collected was evaluated for statistical significance using an unpaired t-test (p value = 0.000586). This indicates that the difference observed in chamber [CO_2] is statistically significant. A greater consumption of carbon dioxide can be attributed to an increased rate of photosynthesis as explained in the following section. Screening inhibitory wavelengths light prior to entering photosystems may prevent photoinhibition. Increased efficiency mediated by protective screening correlated to the increased activity of the Calvin Cycle. Because CO_2 is required to fix carbon prerequisites and form sugars, there is a higher demand for it when the Calvin Cycle is progressing at a faster rate. Plants with a continued demand for CO_2, which is due to the surplus of products from the electron transport chain, will uptake a larger amount of CO_2 from the environment at a greater rate than plants with a lower production of NADPH and ATP. Prior research indicated that increased CO_2 absorption was directly proportional with the quantum efficiency of Photosystem 1 and 2. (Harbinson *et al.*, 1990).

Wavelengths create a continued demand for CO_2 due to the continued of more products from the electron transport chain to the Calvin Cycle. The increased consumption of CO_2 observed in regression models of collected data (Eq. 2-3) results an increased development of sugar, meaning that there is an increased organization of light to chemical energy.

Biomass and interpretation of the data

A higher proportion of biomass relative to the plant's weight correlates with a higher rate of photosynthesis due to the increased storage of organic molecules from photosynthetic processes. Biomass is a key indicator of photosynthetic activity, as it provides insight to the allocation of carbon-based products that were formed during photosynthesis. Bouman and Sylliboy (2012) demonstrated that increased biomass acquisition resulted in a larger leaf surface area and chlorophyll content, contributing to increased photosynthetic activity. The data collected in the biomass acquisition process allows for a cross-check of CO_2 assimilation data to determine a relationship between sequestration rate and biomass. Plants were incubated at 60 degrees Celsius, and their weights were recorded every 24 hrs. Once the observed weight remains constant in between incubation cycles, the final biomass was indicated. The reorganization of energy at face value, is the objective of photosynthesis: to convert energy into a usable form that can support organism growth and development. The trends observed within CO_2 assimilation testing are also observed in the biomass data collected table 4.

Table 4: Weight of betacyanin producing plants and betacyanin producing plants (g) during 24-hour intervals at 60°C

Initial weight (g)	Weight at 24 hrs (g)	Weight at 48 hrs (g)	Weight at 72 hrs (g)	Weight at 96 hrs (g)	Percent biomass (%)
Betacyanin producing plants					
4.4	0.4	0.4	0.4	0.4	10.5
5.8	0.6	0.6	0.6	0.6	11.1
6.2	0.6	0.5	0.5	0.5	8.4
6.0	0.5	0.4	0.4	0.4	7.7
Non-treated plants					
8.2	0.6	0.6	0.6	0.6	.3
9.0	0.5	0.5	0.5	0.5	6.5
5.2	0.3	0.3	0.3	0.3	7.4
4.1	0.2	0.2	0.2	0.2	6.0

The data was normalized through a derivation of biomass composition (see rightmost column). This acts as a normalization procedure to standardize data to a single unit. Since the initial weight differed among the samples, normalization was necessary. To validate if the use of this procedure was appropriate, an unpaired t test was conducted on the initial weights of the samples analyzed. The unpaired t test yielded the p-value of 0.4223. This p-value, above the 0.05 critical value, is considered insignificant, thereby attributing such variation to random chance as opposed to an external stimulus. Next, the unpaired t-test was used to evaluate the statistical significance of percent biomass composition, yielding a p–value of 0.0242. This indicates statistical significance of the difference in biomass composition between the experimental and control samples.

Additionally, the proportion of biomass shared a direct relationship with the rate of CO_2 sequestration, demonstrating the correlation between the assays conducted. The plant # delimiting each row of the CO_2 assimilation data table also correlates with the data present above. This phenomenon establishes a direct correlation between the average amount of CO_2 sequestered and the percent composition of biomass. Shaobing *et al.*, (1991) demonstrated that leaf photosynthetic rate positively correlated with total biomass, further supporting the importance of biomass acquisition in this work. This system demonstrates that plants which received the treatment showed increased biomass acquisition, indicating increased photosynthetic activity.

In conclusion, this research provides a solution to the inefficiencies in photosynthesis through in vivo pigment synthesis, specifically the creation of betacyanin: a novel approach to increase photosynthetic efficiency in *L. sativa*. The assays conducted were conducted with the objective of determining the pigment's role and evaluating the implications of its expression externally. The experimentation conducted also helped validate the different tests that composed the methodology. The increased betacyanin-mediated absorbance of stressor wavelengths, CO_2 assimilation, and the biomass composition of betacyanin-producing samples were statistically significant, supporting the objective of this research. This research exhibited the impact of in vivo betacyanin synthesis in *L. sativa* samples, which can be extended into the carbon capture space for sustainable sequestration. Such enhancement procedures hold the key to the democratization of carbon capture, while preventing the associated environmental degradation associated with DACC. Further investigations stemming from this work would involve a insertion of the 35S RUBY plasmid into the chloroplast DNA (cDNA) through CRISPR Cas9. This would allow for a more frequent exhibition of ROS-scavenging properties, which were outside the scope of this work. Antioxidant properties are a defining characteristic of the Betalain family, warranting their exploration in a photosynthetic context. High Performance Liquid Chromatography (HPLC) would also be implemented to equalize the concentrations of pigments evaluated. Despite the use of ANCOVA to account for differences in pigment dispersion, experimental methods would ensure consistency throughout spectrophotometry.

References

1. Barta C., Kálai T., Hideg K., Vass I. and Hideg É. 2004. Differences in the ROS-generating efficacy of various ultraviolet wavelengths in detached spinach leaves. Functional Plant Biol., 31(1): 23.
2. Bassham A.J., Lambers H and Hans. 2025. Photosynthesis definition, formula, process, diagram, reactants, products, and facts. Encyclopedia Britannica. Available at: https://www.britannica.com/science/photosynthesis/Energy-efficiency-of-photosynthesis
3. Bouman O.T. and Sylliboy J. 2012. Biomass allocation and photosynthetic capacity of willow (Salix spp.) bio-energy varieties. Forstarchiv 83(4): 139–143.
4. Cardona T. Shao S. and Nixon P.J. 2018. Enhancing photosynthesis in plants: The light reactions. Essays Biochemi., 62(1): 85–94.
5. Chen N., Yu Z.H. and Xiao X.G. 2017. Cytosolic and nuclear co-localization of betalain biosynthetic enzymes in tobacco suggests that betalains are synthesized in the cytoplasm and/or nucleus of betalainic plant cells. Frontiers Plant Sci., 8.

6. Chincinska I.A. 2021. Leaf infiltration in plant science: Old method, new possibilities. Plant Methods 17(1).
7. Choquet Y. and Wollman F.A. 2023. The assembly of photosynthetic proteins. Elsevier eBooks, pp. 615–646.
8. Deutz S. and Bardow A. 2021. Life-cycle assessment of an industrial direct air capture process based on temperature–vacuum swing adsorption. Nature Energy 6(2): 203–213.
9. Donkor E F, Ohene-Asare D and Adjei R R. 2020. Association and variability studies for yield and yield components of robusta coffee hybrids (*Coffea canephora*). J. Genet. Genom. Plant Breed., 4(3): 103–111.
10. Goh C.H., Ko S.M., Koh S., Kim Y.J. and Bae H.J. 2011. Photosynthesis and environments: Photoinhibition and repair mechanisms in plants. J. Plant Bio. 55(2): 93–101.
11. Grewal P.S., Modavi C., Russ Z.N., Harris N.C. and Dueber J.E. 2017. Bioproduction of a betalain color palette in Saccharomyces cerevisiae. Metabolic Engin., 45: 180–188.
12. Harbinson J., Genty B. and Baker N.R. 1990. The relationship between CO_2 assimilation and electron transport in leaves. Photosynthesis Res., 25(3): 213–224.
13. Hasanuzzaman M., Bhuyan M.H.M.B., Parvin K., Bhuiyan T.F., Anee T.I., Nahar K., Hossen S., Zulfiqar F., Alam M. and Fujita M. 2020. Regulation of ROS metabolism in plants under environmental stress: A review of recent experimental evidence. Int. J. Mo. Sci., 21(22): 8695.
14. Jaboulay C., Godeux A.S., Doublet P.. and Vianney A. 2021. Regulatory networks of the T4SS control: From host cell sensing to the biogenesis and the activity during the infection. J. Mol. Bio., 433(9): 166892.
15. Kataria S., Guruprasad K.N., Ahuja S. and Singh B. 2013. Enhancement of growth, photosynthetic performance and yield by exclusion of ambient UV components in C_3 and C_4 plants. J. Photochem.Photobio. B: Bio., 127: 140–152.
16. Lacroix B. and Citovsky V. 2019. Pathways of DNA transfer to plants from Agrobacterium tumefaciens and related bacterial species. Annual Revi. Phytopatho., 57(1): 231–251.
17. Peng S., Krieg D.R. and Girma F.S. 1991. Leaf photosynthetic rate is correlated with biomass and grain production in grain sorghum lines. Photosynthesis Res. 28(1): 1–7.
18. Pramanik D., Lee K. and Wang K. 2024. A simple and efficient method for betalain quantification in RUBY-expressing plant samples. Frontiers Plant Sci., 15.
19. Rees D.C., Johnson E. and Lewinson O. 2009. ABC transporters: The power to change. Nature Revi. Mol. Cell Bio. 10(3): 218–227.
20. Sadowska-Bartosz I. and Bartosz G. 2021. Biological properties and applications of betalains. Molecules 26(9): 2520.
21. Solovchenko A.E. and Merzlyak M.N. 2008. Screening of visible and UV radiation as a photoprotective mechanism in plants. Russian J. Plant Physio., 55(6): 719–737.
22. Tiseo I. 2025. Annual global emissions of carbon dioxide 1940–2024. Statista. Available at: https://www.statista.com/statistics/276629/global-co2-emissions/
23. Wargent J.J., Elfadly E.M., Moore J.P. and Paul N.D. 2011. Increased exposure to UV-B radiation during early development leads to enhanced photoprotection and improved long-term performance in Lactuca sativa. Plant Cell Environ., 34(8): 1401–1413.